

# Effect of Piles on the Design of Raft Foundation



L. M. Malavika, V. Balakumar, and S. S. Chandrasekaran

**Abstract** The combined raft, soil and pile foundation system has reached a high level of familiarity and is now being used to support a large number of structures. When the bearing capacity of the raft foundation is acceptable but the settlement value exceeds the permissible limit, raft-soil system is reinforced with piles to reduce settlement. Here, piles act as settlement reducers to the raft-soil foundation system. Different researchers have studied the effect of varying pile, raft and soil parameters on the settlement response and load-sharing behaviour of the raft and piles in a combined raft, soil and pile foundation system but less attention has been paid to the stress response behaviour of the raft. As this aspect is considered to be important from economics of raft design, a study has been performed to understand the stress response of the raft on the introduction of piles. The stress response of the raft for varying load conditions,  $E_c/E_s$  ratios, thicknesses of raft and diameters of pile have been studied by performing numerical analyses on the foundation system supporting a moderately loaded 12-storeyed real-time commercial structure located in Chennai, India. An attempt has been made to study the applicability of Equivalent Pier concept. The above analyses were performed for two different layouts of piles. The behaviour of the stress and settlement responses of the raft reinforced with piles was compared with unpiled raft. Staad-Pro V8i and Ansys 16.0 have been used for the study and this paper presents observations and discussions from the study.

**Keywords** Raft reinforced with piles · Raft stress response · Raft settlement response · Equivalent pier

---

L. M. Malavika (✉)  
VIT, Vellore, Tamil Nadu, India  
e-mail: [lingashetty.malavika@gmail.com](mailto:lingashetty.malavika@gmail.com)

V. Balakumar  
Simplex Infrastructures Limited, Chennai, Tamil Nadu, India

S. S. Chandrasekaran  
Department of Structural & Geotechnical Engineering, VIT, Vellore, Tamil Nadu, India

## 1 Introduction

Exponential growth in infrastructure development has forced the designers to accept any ground condition irrespective of its nature. The foundation system must satisfy the serviceability and ultimate limit state conditions and also be viable economically in spite of the ground conditions. The economics of the raft design lies in designing the foundation such that the factor of safety against bearing capacity failure is at the minimum specified value and the total settlement is less than the permanent settlement.

Rafts are designed for the required bearing capacity, however, when the bearing capacity of the raft foundation is acceptable but the settlement values exceed beyond the permissible limits, the raft-soil system is reinforced with piles to reduce settlement (Zeevaert 1957). Here, piles act as settlement reducers to the raft-soil foundation system.

Extensive research had been performed by various researchers to understand the settlement reduction in raft on the introduction of piles (Poulos 1994a, b). Various raft, soil and pile parameters that affect the settlement response and the load-sharing behaviour of the raft and piles in a combined raft, soil and pile foundation system had been also studied extensively. However, very little research has been performed to study the effect of introducing piles on the raft stress response and bending moment. Therefore, it becomes a necessity to study the behaviour of raft stresses on the introduction of piles in a raft-soil foundation system for an effective and economical design since the economy of a foundation lies in both optimum pile layout and provisions in raft.

## 2 Objective

The main objective of this study is to determine the effect of reinforcing the raft-soil system with piles on the raft stresses and bending moment.

## 3 Methodology

In the present study, a twelve-storied commercial building resting on a raft-soil foundation system reinforced with piles has been adopted. The structure was analysed in Staad-Pro to obtain the column reactions. These column reactions act at the base of the structure. The linear soil-structure interaction analysis of the combined raft-soil and pile foundation system was performed using Ansys Workbench 16.0.

The behaviour of the raft stress and settlement response was studied by plotting graphs and contours for four different conditions obtained by varying parameters like Young's modulus of soil ( $E_s$ ), Pile diameter ( $D$ ), Raft thickness ( $t$ ) and type of

loading. The above analyses were performed for two different pile layouts. The stress response for the pile reinforced raft was compared with unpiled raft. An attempt was made to study the applicability of Equivalent Pier concept (Balakumar et al. 2013a, b). Effort was made to know if there was any variation in the raft stress response.

### 3.1 Structural Analysis

The shape of the twelve-storied commercial building is irregular with a width of 27.38 m and a length of 41.2 m along the largest span. The building lies on a raft—soil foundation system reinforced with piles. The dimensions of the raft are same as the shape of the building. Figures 1 and 2 shown below represent the floor plan and

Fig. 1 Floor plan

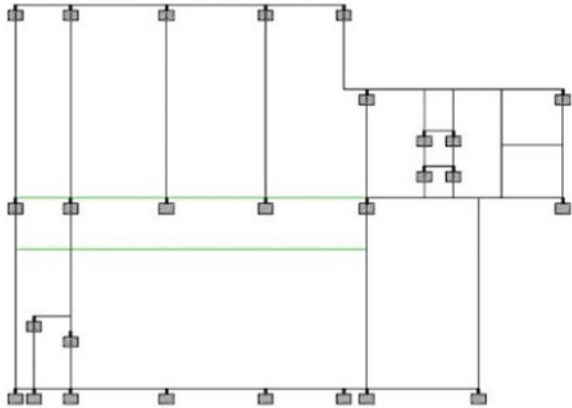
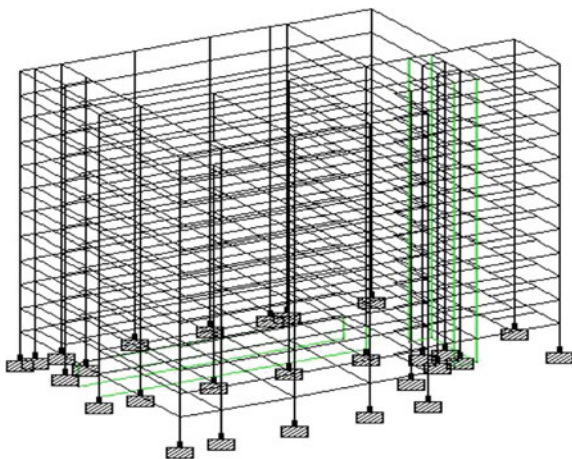


Fig. 2 Structural frame



**Table 1** Physical properties of model

Specification	Value (mm)
Slab thickness	200
Size of beams along lateral direction	800 × 750
Size of beams along transverse direction	450 × 600
Size of columns	800 × 800
Outer wall thickness	230
Inner wall thickness	230
Storey height	3750
Number of storeys	12

the structural frame of the twelve-storied building respectively. Table 1 presents the dimensions of the physical components of the twelve-storied building.

The framed model is subjected to a combination of Dead load (D.L.) and Live load (L.L.). Three-dimensional analysis has been performed to obtain the support reactions. These reactions obtained at the base of the structure act as the structural load on the foundation.

### 3.2 Numerical Analysis

In the case of Staad-Pro, it is a known fact that geotechnical problems cannot be handled. Although some approximations can be done, the applications are very limited like preliminary analysis of retaining walls which is conforming to beam elements. Since the soil cannot be modelled, Ansys was chosen to do the soil–structure interaction studies. The physical and material properties of the combined foundation system are mentioned in Tables 2 and 3, respectively.

The pile length of 0.8 times the least dimension of the raft (B) was chosen since it is the optimum limit beyond which the piles do not possess additional bearing capacity (Cooke 1986; Balakumar 2008). Figures 3 and 4 show the individual raft and pile models, respectively.

In the case of unpiled raft, shown in Fig. 5, the depth of the soil block is taken as 2.5 times the least dimension of the raft (B) and both the length and width of the soil block as 3 times the least dimension of the raft (B). This is due to the reason that the impact

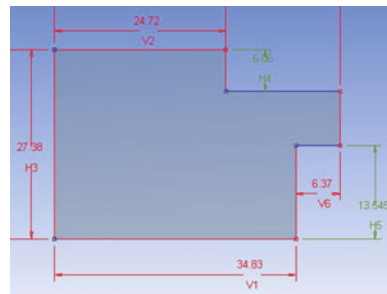
**Table 2** Physical properties of raft, piles and soil

Property	Raft	Piles	Soil
Material	M25 concrete	M25 concrete	Medium dense sand
Shape	Irregular	Circular	Cube
Depth	1 m	24 m	68.45 m
Width	27.38 m	0.9 m	82.14 m

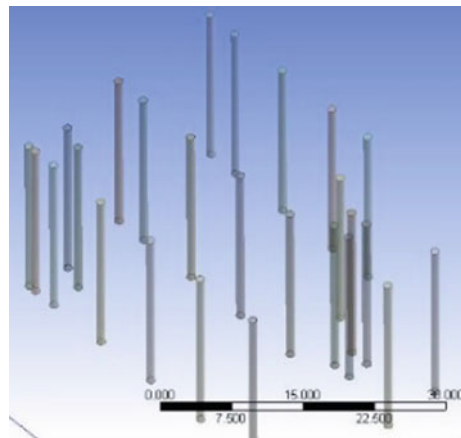
**Table 3** Material properties of raft, piles and soil

Property	Raft	Piles	Soil
Material	Concrete	Concrete	Sand
Compressive strength (kN/m <sup>2</sup> )	27579	27579	–
Elastic modulus (Pa)	$3 \times 10^{10}$	$3 \times 10^{10}$	$3 \times 10^6$
Density (kN/m <sup>3</sup> )	22.54	22.54	15.5
Poisson ratio	0.18	0.18	0.3
Shear angle	–	–	$33^0$

**Fig. 3** Raft

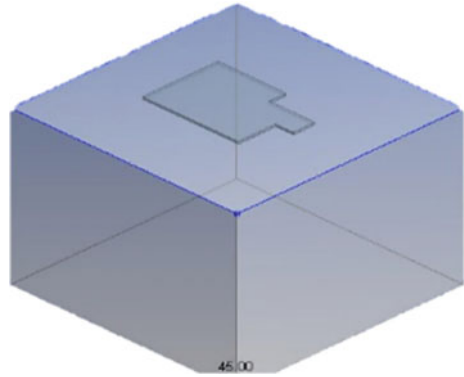
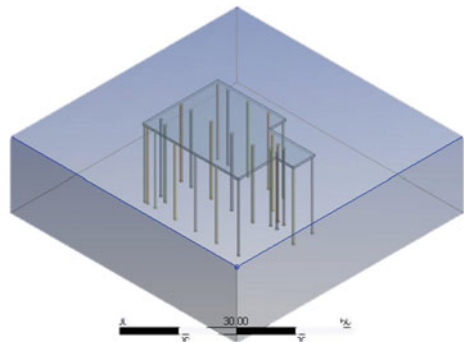


**Fig. 4** Piles



of the raft does not exceed these limits in the surrounding soil (Balakumar 2008). Figure 6 represents the raft reinforced with piles in the raft-soil system wherein the depth of the soil is taken equal to the length of the piles to provide contact between the tip of the piles and the bottom of the soil surface.

Perfect contact is provided between raft—soil, raft—piles and piles—soil (Balakumar 2008). The accuracy of the analysis depends upon meshing and continuity of the elements in the nodes. Hence, in generation of mesh, extreme care was

**Fig. 5** Unpiled raft in soil**Fig. 6** Raft with piles in soil

taken to ensure identical mesh refinement patterns for different analytical cases under comparison. A 2-m uniform quadrilateral mesh was provided throughout the entire foundation system.

Fixed boundary conditions are provided at the bottom surface and along the four edges of the soil block (Balakumar 2008). The fixity conditions act as bounding limits to the soil. The loads are imposed on the raft and the settlement and stress values are obtained after the analysis. The values thus obtained at each node along the orthogonal directions of the raft at the centre and the edge are used in plotting the graphs.

**Type of loading.** The column loads at the base of the structure were given as two different types of input for soil–structure interaction analysis in Ansys Workbench. They are as follows:

- Concentrated loads
- Equivalent uniformly distributed load of 157.766 kN/m<sup>2</sup>

Figures 7 and 8 show the type of loading imposed on raft. Initially, the unpiled raft (Case–A) was subjected to concentrated load as well as equivalent UDL for  $E_c/E_s$  ratios of 10,000, 2,000, 1,500, 1,200, 1,000 and 100.

**Fig. 7** Point load on raft

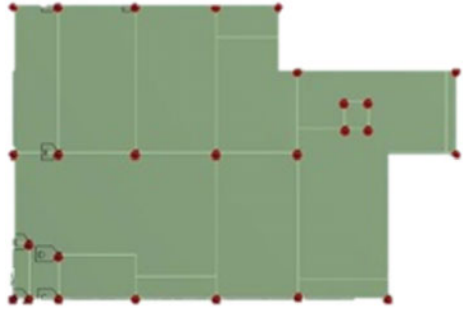


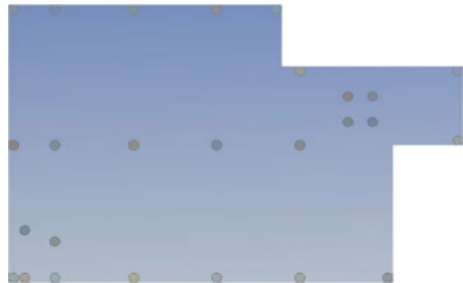
**Fig. 8** Uniformly distributed load on raft

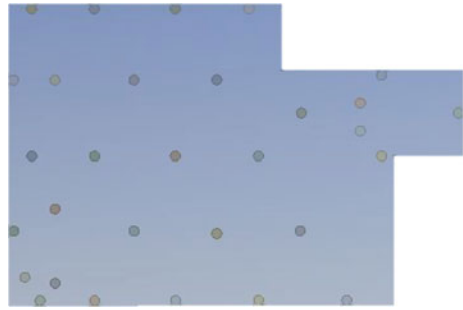


Later, the piles were introduced below the raft in two different layouts, one layout with piles located below the position of the columns under the raft (Case–B) and the other layout with piles located in between the position of the columns under the raft (Case–C). Figures 9 and 10 represent the different pile layouts.

Table 4 presents a comparison for the maximum settlement between cases A, B and C subjected to PL and UDL, respectively. It can be seen that the total settlement exceeds the permissible limits in all cases except for one case where there is an extreme reduction in the maximum settlement in the unpiled raft when the  $E_c/E_s$  ratio is equal 100. This is because the  $E_c/E_s$  ratio equal to 100 indicates a very dense and stiffer soil condition. Such a stiffer and denser soil possesses a very high

**Fig. 9** Case B



**Fig. 10** Case C**Table 4** Comparison of settlement in cases A, B and C

Ec/Es	Max. settlement under PL (mm)			Max. settlement under UDL (mm)		
	Case A	Case B	Case C	Case A	Case B	Case C
10,000	1347.0	1079.3	1028.7	1160.8	694.0	694.4
2,000	309.0	356.1	356.7	255.0	166.3	167.1
1,500	297.0	294.0	266.7	194.2	132.7	132.3
1,200	192.9	253.9	228.0	158.0	111.9	111.4
1,000	300.7	225.6	200.6	131.9	97.3	96.7
100	20.3	50.8	49.8	138	13.6	5.9

bearing capacity and hence the raft-soil foundation system in such dense soil shows less settlement. Designing the raft for such maximum settlement values will make the design uneconomical. This necessitates the introduction of settlement-reducing piles.

It was also observed from Table 4 that the introduction of piles in the raft-soil system has reduced the total settlement to about 25–45% on an average. This validates the purpose of the addition of piles as settlement reducers to the raft-soil foundation system.

It can be seen from Table 4 that the settlement reduction is maximum for Ec/Es equal to 10,000 and it decreases with an increase in Ec/Es ratio. This is because piles are fully frictionized when Ec/Es is equal to 10,000 but as the Ec/Es ratio decreases, the soil becomes denser and the capacity of the piles to turn into friction piles reduces (Cooke 1986).

A considerable difference was observed in the settlement contour pattern under PL and UDL conditions for all the three cases. This is because of the variation in the type of loading. In the case of raft-soil foundation system subjected to PL, the contact pressure varies due to variation in loads and hence the settlement profile also varies accordingly as seen in Fig. 11.

In the case of UDL, there is uniform contact pressure distribution throughout the area of the raft due to the uniformity in loading. This resulted in a more uniform settlement contour as seen in Fig. 12. Figure 13 indicates that the effect of raft



**Fig. 11** Settlement contour under point load

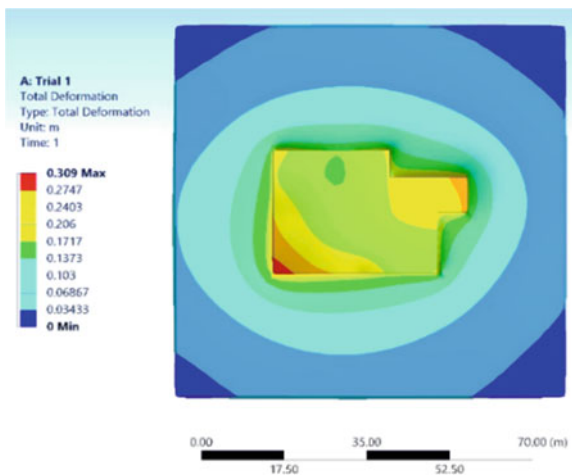


**Fig. 12** Settlement contour under UDL

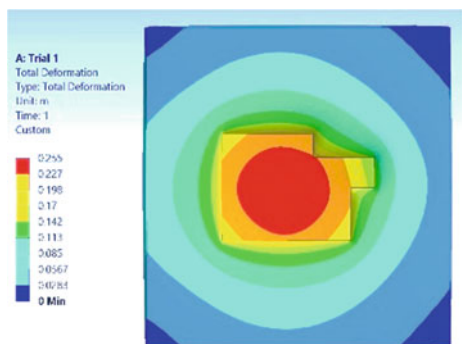


**Fig. 13** 3D view—Settlement contour

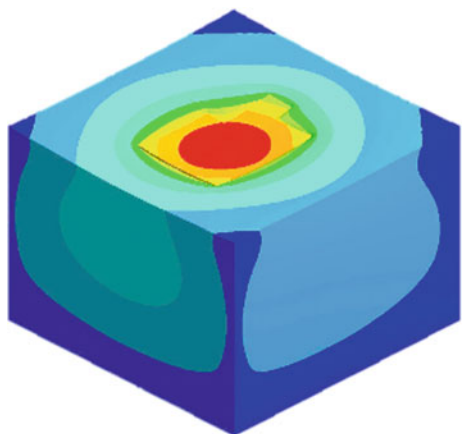


**Fig. 14** Settlement under UDL for Case B

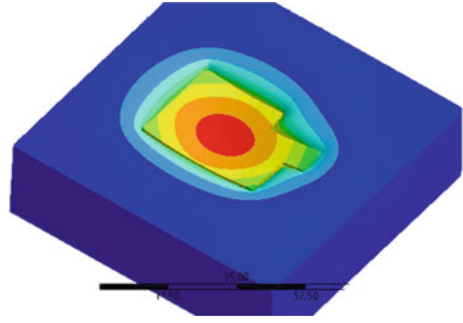
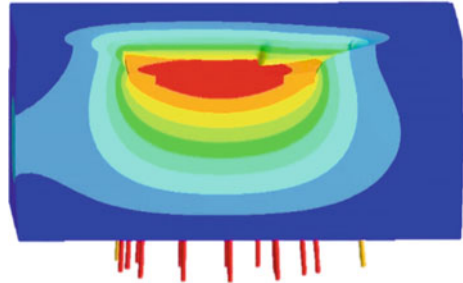


**Fig. 15** Section view of contour



settlement is negligible at the bottom and at the edge of the soil which justifies that the impact of the raft is limiting in the soil as discussed in Sect. 3.2.

Figures 14 and 15 represent the settlement contours for complete and section views of a combined raft, soil and pile foundation system under UDL for case B, respectively. It can be seen from Figs. 12 and 14 that the settlement pattern remains identical but vary in magnitude.

Figure 15 shows the settlement contour along the depth of the foundation. The maximum settlement occurs at the centre as well as the tip of the piles. This denotes the transfer of the load to the surrounding soil through the tip of the piles from the centre portion of the raft.

The settlement of the raft along the orthogonal grids was obtained and graphs have been plotted to present a comparison for the settlement in Cases A, B and C when subjected to PL and UDL. Figures 16 and 17 present a comparison between cases A and B for the raft settlement along the transverse grid when subjected to PL and UDL for a ratio of  $E_c/E_s$  equal to 2,000.

It can be observed from Figs. 16 and 17 that the settlement pattern for unpiled raft and piled raft subjected to PL and UDL are similar, respectively, but the raft reinforced with piles exhibited much lesser settlement compared to unpiled raft. This validates that the piles act as settlement reducers in raft-soil system.

It can be seen from the above settlement graphs that the settlement trend curve for foundation system subjected to UDL showed a concave profile with maximum settlement at the centre reflecting the nature of the raft mainly flexible raft. But under

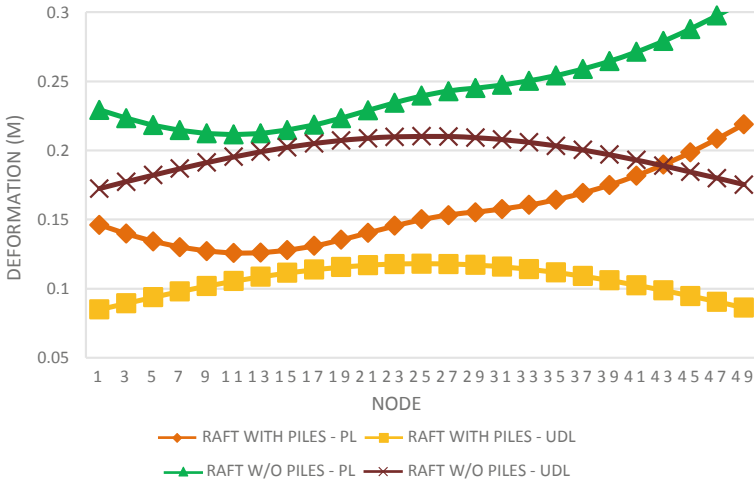


Fig. 16 Settlement graph for cases A and B—Outer Grid

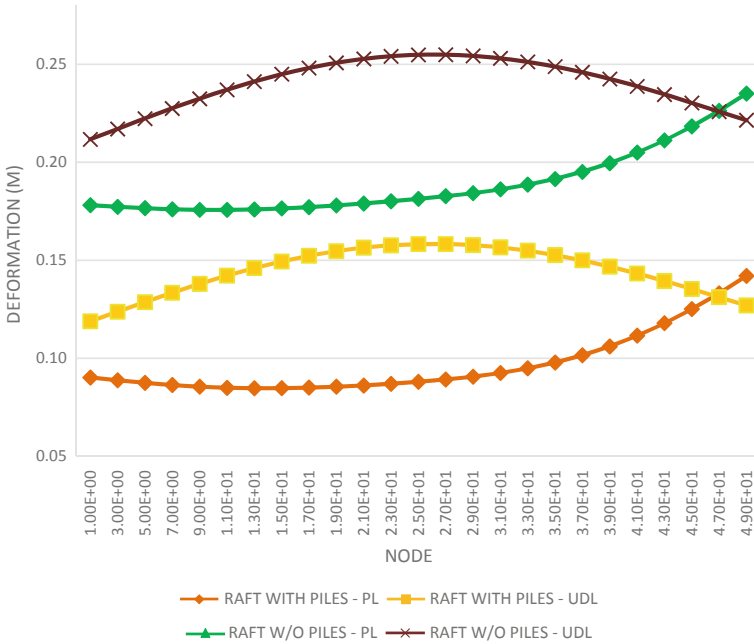


Fig. 17 Settlement graph for cases A and B—Central Grid

the same condition, when the load is considered as PL, the outer and central grids show a reversal in shape due to their dependence on the individual column load. Similar graphs were plotted for all other cases for different  $E_c/E_s$  ratios and it was observed that the raft settlement response remained same but varied in magnitude. It was observed that the deformation reduced from 45–55% at the edges and 40–45% at the centre of the raft on introduction of piles.

Similar to settlement profile, Table 5 presents a comparison between the maximum stress values of the combined foundation system subjected to PL and UDL for different  $E_c/E_s$  ratios. It can be seen from Tables 5 and 6 that the maximum stress value remained same for unpiled rafts subjected to PL for all the  $E_c/E_s$  ratios whereas the maximum stress value varied for unpiled rafts subjected to UDL. In the case of foundation system subjected to PL, the stresses were concentrated in the raft area subjected to high concentrated loads whereas under UDL, the stresses were redistributed throughout the entire area of the raft due to uniformity in the distribution of loads. It can also be seen that the maximum stress value decreased with a decrease in the  $E_c/E_s$  ratio. As the  $E_c/E_s$  ratio decreases, the soil becomes denser leading to less deformation and eventually lesser stresses in the raft.

Similar to the raft settlement response, a variation in the stress contours of unpiled rafts subjected to PL was observed. Figures 18 and 19 represent the stress contours in the unpiled raft-soil foundation subjected to UDL for  $E_c/E_s$  ratio equal to 2,000.

From Fig. 18, it can be observed that the raft stresses are concentrated more at the centre portion of the raft and are negligible at the edges. Since the settlement is

**Table 5** Maximum stress under point load (Pa)

Ec/Es	Maximum stress under point load (Pa)		
	Case A	Case B	Case C
10,000	$11.28 \times 10^7$	$11.24 \times 10^7$	$11.28 \times 10^7$
2,000	$11.29 \times 10^7$	$11.21 \times 10^7$	$11.29 \times 10^7$
1,500	$11.29 \times 10^7$	$11.25 \times 10^7$	$11.29 \times 10^7$
1,200	$11.29 \times 10^7$	$11.25 \times 10^7$	$11.29 \times 10^7$
1,000	$11.28 \times 10^7$	$11.25 \times 10^7$	$11.29 \times 10^7$
100	$11.29 \times 10^7$	$11.25 \times 10^7$	$11.29 \times 10^7$

**Table 6** Maximum stress under uniformly distributed load (Pa)

Ec/Es	Maximum stress uniformly distributed load (Pa)		
	Case A	Case B	Case C
10,000	$2.91 \times 10^7$	$3.39 \times 10^7$	$2.65 \times 10^7$
2,000	$1.21 \times 10^7$	$1.43 \times 10^7$	$1.28 \times 10^7$
1,500	$0.99 \times 10^7$	$1.05 \times 10^7$	$1.06 \times 10^7$
1,200	$0.85 \times 10^7$	$0.89 \times 10^7$	$0.90 \times 10^7$
1,000	$0.74 \times 10^7$	$0.77 \times 10^7$	$0.77 \times 10^7$
100	$0.12 \times 10^7$	$0.13 \times 10^7$	$0.12 \times 10^7$

**Fig. 18** Stress contour in unpiled raft under point load

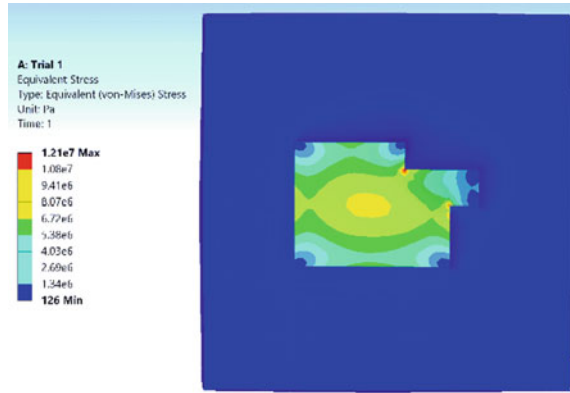
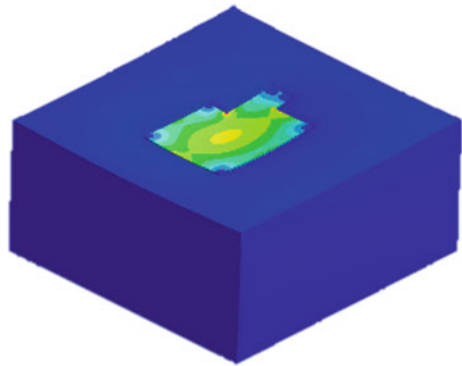


**Fig. 19** Stress contour in soil



more at the centre of the raft, the stresses are highly concentrated at the centre. This trend in stress variation is similar to the settlement response of the unpiled raft when subjected to UDL as seen in Fig. 14. It can be seen from Fig. 19 that the stresses in the soil are negligible.

The stress contours at the section of the unpiled raft were obtained to study the stress pattern along the depth of the foundation. The stresses in the soil were negligible for all the three cases as discussed previously.

It can be seen from Fig. 20 that the raft stress is minimum at the centre and maximum at the top and bottom of the unpiled raft under UDL. The raft design can therefore be optimized accordingly with respect to raft stress and settlement behaviour.

The variation in stresses means that the Bending Moment (B.M.) and Shear Force (S.F.) will also vary along the raft area. Hence it becomes important to study the stress response behaviour of the raft from the view of the economics of the raft.

Figure 21 represents the stress variation at the bottom surface of the piled raft. It can be observed that the stress varies uniformly along both the orthogonal directions of the surface of the raft. Similar stress trend was observed in Cases B and C but with

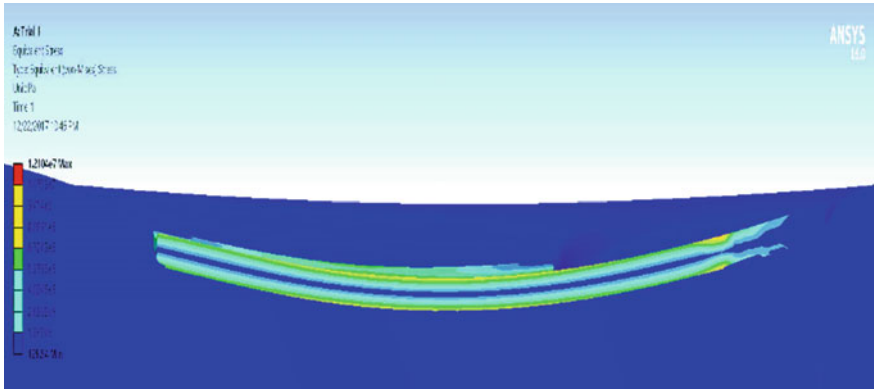


Fig. 20 Section contour for stresses in case A under UDL

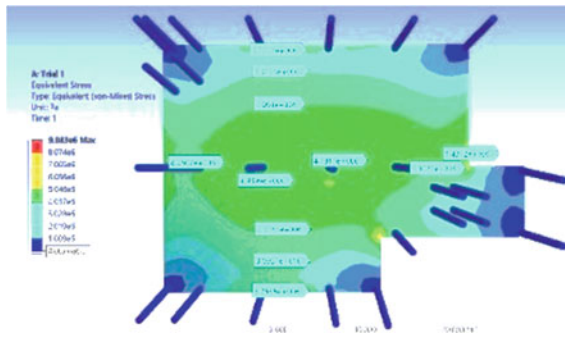


Fig. 21 Stress contour at the bottom of raft

a variation in magnitude under PL and UDL for different  $E_c/E_s$  ratios. The stress in piles was observed to be minimum in all cases as seen in Fig. 22.

Figures 23, 24 and 25 represent the stress in piles. It can be observed that stress in the area of raft-pile contact is maximum. This is due to the transfer of raft stress to the piles. The stress in the piles is maximum at the head and it reduces with an increasing depth in the piles as indicated in Figs. 22 and 23. Variation of stress indicates a variation in the B.M. and shear forces. Hence, the reinforcement in the raft can be optimized by designing it in areas of higher stresses leading to an economical design.

Graphs have been plotted for raft stresses at the bottom surface in cases A, B and C and a comparison has been made between them to study the raft stress behaviour. Figures 26 and 27 present a comparison between the unpiled and piled raft stresses at the bottom surface area of the raft for  $E_c/E_s$  equal to 2,000.

It was observed from the stress response graphs of the raft that the stress response pattern although remains similar in trend under UDL, it has a pronounced variation particularly in the case of outer grids. This is mainly due to the varying magnitude

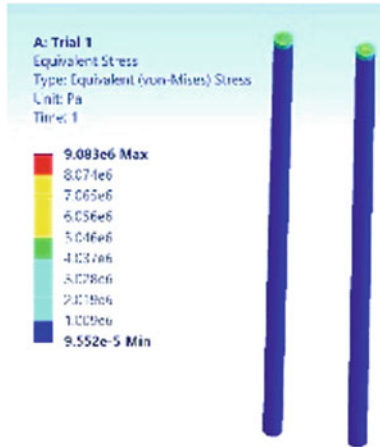


Fig. 22 Stress contour in piles

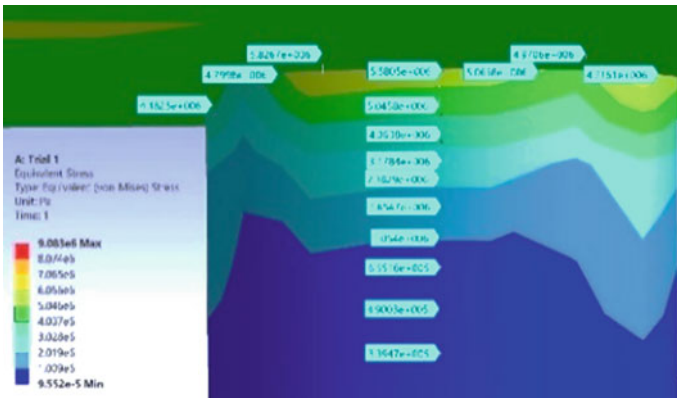


Fig. 23 Stress contour at raft-pile contact area

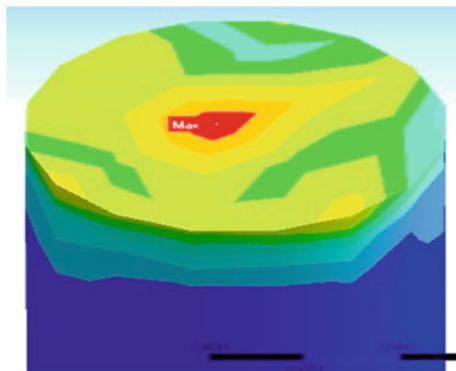


Fig. 24 Stress contour at head of the pile

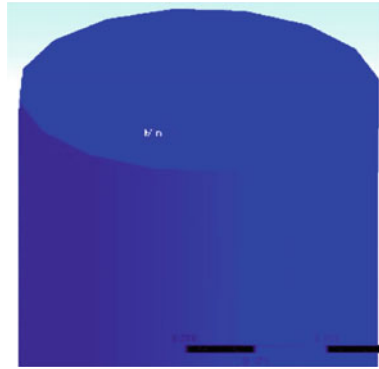


Fig. 25 Stress contour at pile tip

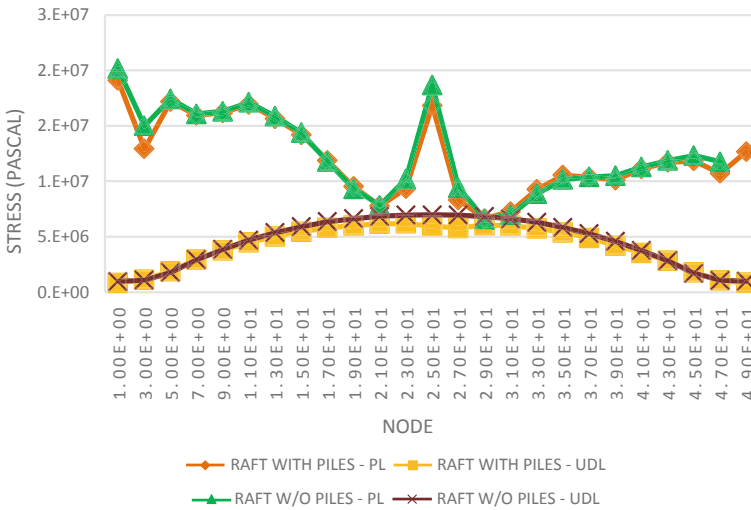


Fig. 26 Stress graph along the outer grid of the raft in transverse direction

of the column load. The upper peaks in the stress trend curves under PL reflect the concentration of raft stresses at the pile locations. The transfer of stresses from the raft to the piles occurs here as mentioned previously. The lower peaks reflect the raft between the piles. In the present structure, columns are very widely spaced, therefore, the stress pattern under the PL follows the same pattern.

Similar graphs were plotted for all other cases for different  $E_c/E_s$  ratios and it was observed that the stress pattern remained same but with a variation in magnitude. It was observed that the stress value reduced from 7–15% at the edges and 10–20% at the centre of the raft due to the introduction of piles in the raft.

Thus, it can be concluded that the method of applying loads influences the displacement and stress patterns. It was observed that the displacement and stress



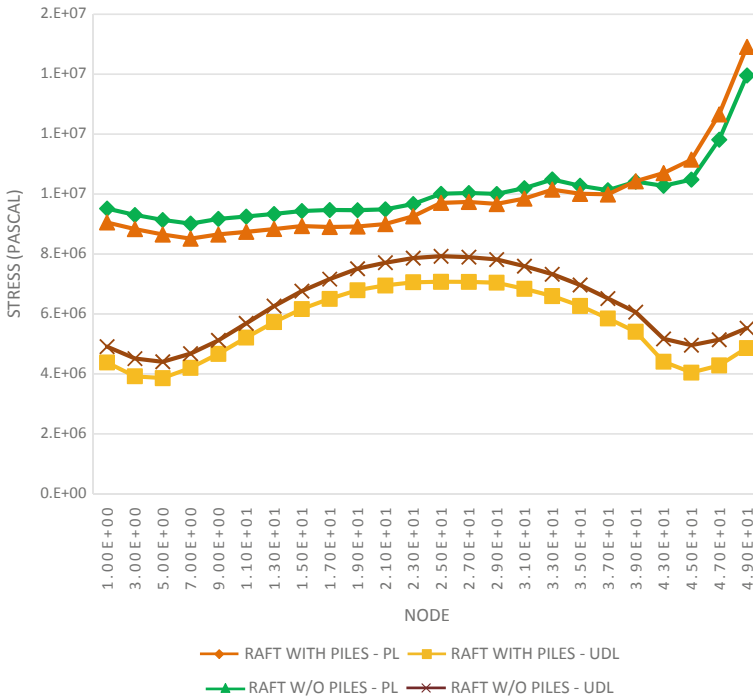


Fig. 27 Stress graph along the central grid of the raft in transverse direction

patterns were identical for all the three cases with a pronounced reduction in magnitude in raft reinforced with piles, i.e. cases B and C. The raft and pile design can be optimized efficiently by studying the settlement and stress responses of the raft and the piles.

**Variation in  $E_c/E_s$ .** In the present case, numerical analyses were performed on an unpiled raft of thickness 1 m located at a depth of 3 m from the ground surface. Retaining wall was considered around the raft. A pressure of 111276 Pa was obtained by deducting the surcharge pressure at 3 m depth. Numerical analyses were repeated for cases B and C and the results were compared to study the raft behaviour. In the analysis, the  $E_c$  value was kept constant as  $3 \times 10^7$  kN/m<sup>2</sup> whereas the  $E_s$  value was varied. The raft, pile and soil properties mentioned in Tables 2 and 3 were adopted. Table 7 presents a comparison of the stresses in cases A, B and C for varying  $E_c/E_s$  ratios.

From the above table, it can be seen that the stress reduces on the introduction of piles for both the pile layouts. It was observed that the stress contour trend remained similar to unpiled and piled rafts under UDL in previous sections but with a slight variation in magnitude. For the present case, the settlement value for  $E_c/E_s$  ratio equal to 2,000 satisfies the permissible limits. Hence, the ratio of  $E_c/E_s$  equal to 2,000 had been adopted in the further studies.

**Table 7** Comparison of stresses in cases A, B and C

Ec/Es	Maximum stress (in Pa) under a load of 111276 Pa		
	Case A	Case B	Case C
10,000	$2.45 \times 10^7$	$2.39 \times 10^7$	$1.80 \times 10^7$
2,000	$0.95 \times 10^7$	$0.90 \times 10^7$	$0.90 \times 10^7$
1,500	$0.80 \times 10^7$	$0.74 \times 10^7$	$0.74 \times 10^7$
1,200	$0.69 \times 10^7$	$0.63 \times 10^7$	$0.63 \times 10^7$
1,000	$0.57 \times 10^7$	$0.54 \times 10^7$	$0.54 \times 10^7$
100	$0.08 \times 10^7$	$0.09 \times 10^7$	$0.08 \times 10^7$

Graphs were plotted similar to previous section and comparison was made. It was observed that the trend for the settlement and stress responses of the raft varied along a concave profile which was similar to the previous observations but with a variation in magnitude. It was observed that the settlement reduced from 45–55% at the edges and 40–45% at the centre of the raft on the introduction of piles. Similar results were observed for all the other grids under all cases.

Figures 28 and 29 represent the stress response of the raft for cases A and B when  $E_c/E_s$  is equal to 2,000. The raft stresses were obtained at the raft-soil contact surface but on the raft surface. The pattern of stress distribution with piles obtained after analysis was similar to the results published by Balakumar (2008). The slight variation in the stress trend curves as seen in Figs. 28 and 29 is due to the non-uniform spacing of piles.

It was observed from the calculations that the stress value reduced about 7–15% at the edges and 10–20% at the centre of the raft due to the introduction of the piles for both the layouts. At the raft edges, the variation in stress was marginally less compared to the centre. This variation is mainly due to the edge being free and not restrained by retaining walls in actual analysis.

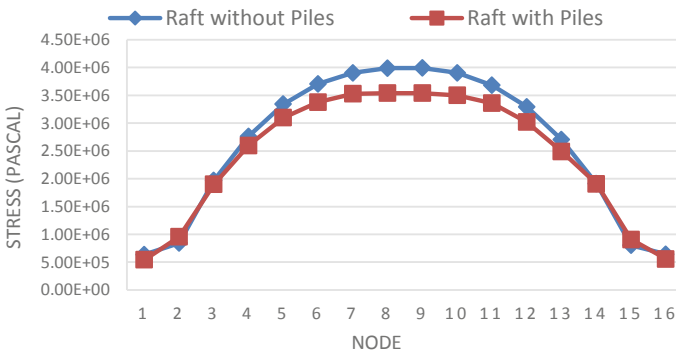


**Fig. 28** Stress graph along outer grid of raft in transverse direction

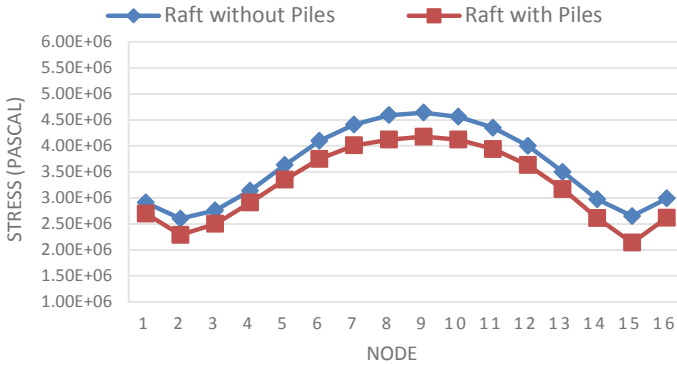


Fig. 29 Stress graph along central grid of raft in transverse direction

**Variation of D/t when pile diameter (D) is kept constant.** In the present case, the numerical analyses were performed on the combined raft, soil and pile foundation system for four D/t ratios, where D is the diameter of the pile and t is the thickness of the raft. The diameter of the piles was kept constant as 0.9 m and the raft thickness was varied. The raft was located at a depth of 3 m from the ground surface and the piles of length 24 m were modelled under the raft beneath the location of the columns. The soil was modelled as a block of medium dense sand condition. A constant  $E_c/E_s$  ratio of 2,000 was adopted to perform all the analyses under the present case, where  $E_c$  was equal to  $3 \times 10^{10} \text{ N/m}^2$  and  $E_s$  equal to  $1.5 \times 10^7 \text{ N/m}^2$ . The results obtained from various analyses of conditions A, B and C were compared with each other.

It was observed that the introduction of piles reduced the settlement for about 23–37%. It was also observed that the reduction in the overall settlement increased with an increase in the raft thickness (Poulos 1998, 2001) for a constant pile diameter.

Table 8 presents a comparison between the maximum stresses for cases A, B and C for varying D/t ratios when D was kept constant. It was observed that there was no much variation between the maximum stress values for cases B and C when the pile diameter was kept constant. It was observed that the settlement and stress trend was similar to previous sections for all the D/t ratios but with a variation in magnitude.

Table 8 Comparison of stresses in cases A, B and C when D is constant

D/t	D (mm)	t (mm)	Maximum stress (Pa)		
			Case A	Case B	Case C
1.2	900	750	$0.90 \times 10^7$	$0.89 \times 10^7$	$0.89 \times 10^7$
1.0	900	900	$0.94 \times 10^7$	$0.92 \times 10^7$	$0.92 \times 10^7$
0.9	900	1000	$0.95 \times 10^7$	$0.90 \times 10^7$	$0.90 \times 10^7$
0.8	900	1125	$0.94 \times 10^7$	$0.86 \times 10^7$	$0.86 \times 10^7$

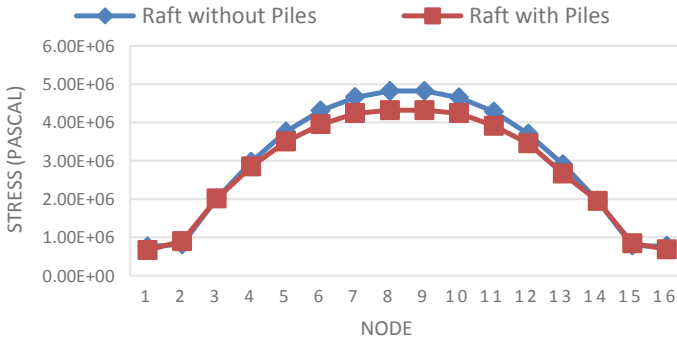


**Fig. 30** Stress graph along outer grid of raft in transverse direction

It was observed that the deformation reduced for about 45–55% at the edges and 40–45% at the centre of the raft on introduction of piles.

Graphs were plotted to compare the raft stress response for cases A, B and C for varying D/t ratios when D was kept constant. Figure 30 represents the stress response behaviour of the raft for a D/t ratio of 1.2. The stress value reduced from 7–15% at the edges and 10–20% at the centre of the raft due to the introduction of piles. Similar trend was observed in all the other cases.

**Variation of D/t when raft thickness (t) is kept constant.** In the present case, the numerical analyses were performed similar to the above section but here, raft thickness of 1 m was adopted and kept constant whereas the pile diameter was varied. Table 9 presents a comparison of stresses between cases A, B and C for varying D/t ratios when t was kept constant.

It can be observed from the table that the stresses in the raft under cases B and C increases as the pile diameter decreases for a constant raft thickness. For D/t ratios less than 1.2, i.e. when the pile diameter is less than the raft thickness, there is an increase in the raft stresses. It was observed that the settlement and stress trend was similar to previous sections for all the D/t ratios but with a variation in magnitude.

**Table 9** Comparison of stresses in cases A, B and C when t is constant

D/t	D (mm)	t (mm)	Maximum stress (Pa)		
			Case A	Case B	Case C
2.00	2000	1000	$0.85 \times 10^7$	$0.76 \times 10^7$	$1.42 \times 10^7$
1.75	1750	1000	$0.85 \times 10^7$	$0.81 \times 10^7$	$0.72 \times 10^7$
1.5	1500	1000	$0.85 \times 10^7$	$0.83 \times 10^7$	$0.79 \times 10^7$
1.2	1200	1000	$0.85 \times 10^7$	$0.85 \times 10^7$	$0.86 \times 10^7$
1.0	1000	1000	$0.85 \times 10^7$	$0.90 \times 10^7$	$0.90 \times 10^7$
0.8	800	1000	$0.85 \times 10^7$	$0.91 \times 10^7$	$0.93 \times 10^7$

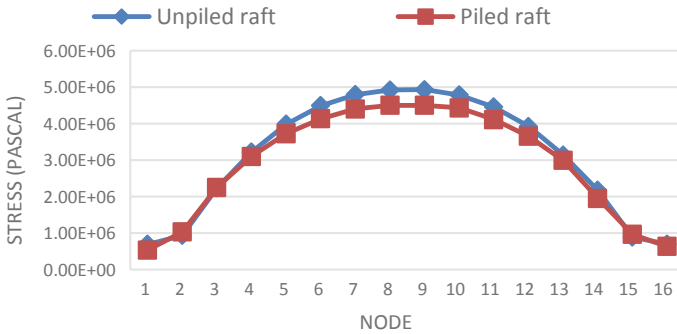


**Fig. 31** Stress graph along central grid of raft in transverse direction

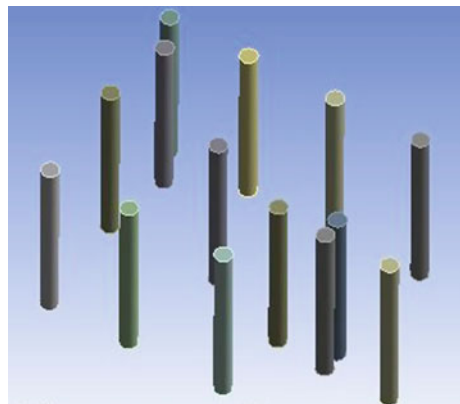
The graph representing the stress response behaviour of the raft was also similar in pattern but varied in magnitude as seen in Fig. 31.

Figure 31 represents the stress response behaviour of the raft for a D/t ratio equal to 1.2. The stress value reduced from 7–15% at the edges and 10–20% at the centre of the raft due to the introduction of piles. Similar trend was observed in all the other cases.

**Equivalent Pier Analysis.** A special case of equivalent pier system has been analysed to study its applicability and influence on the behaviour of raft deformation and stresses. Three equivalent pier analyses have been performed by adopting a raft of thickness 1 m located at a depth of 3 m from the ground surface. Equivalent piles of length 24 m were modelled under the raft surrounded by medium dense sandy soil.  $E_c/E_s$  ratio of 2,000 has been adopted for the analyses. Equivalent pier diameter (Dequ) was calculated. The equivalent piles of 24 m length are shown in Fig. 32.

Tables 10 and 11 present a comparison for the maximum settlement and stresses in a raft between the cases of un-piled raft (Case A), raft reinforced with piles below the position of columns (Case B) and raft reinforced with equivalent piles below the

**Fig. 32** Equivalent Piles



**Table 10** Comparison of maximum deformation

D (m)	t (m)	Dequ (m)	Maximum deformation (mm)				
			Case A	Case B	Case Bequ	Case C	Case Cequ
1.5	1	2.1	135.29	119.13	118.48	117.95	119.19
1.2	1	1.8	134.95	118.97	118.20	118.01	119.08
1.0	1	1.4	119.25	118.81	118.81	117.93	118.87

**Table 11** Comparison of maximum stresses

D (m)	t (m)	Dequ (m)	Maximum stress (Pa)				
			Case A	Case B	Case Bequ	Case C	Case Cequ
1.5	1	2.1	$0.99 \times 10^7$	$0.83 \times 10^7$	$0.83 \times 10^7$	$0.79 \times 10^7$	$0.77 \times 10^7$
1.2	1	1.8	$0.94 \times 10^7$	$0.85 \times 10^7$	$0.84 \times 10^7$	$0.86 \times 10^7$	$0.86 \times 10^7$
1.0	1	1.4	$0.92 \times 10^7$	$0.90 \times 10^7$	$0.90 \times 10^7$	$0.90 \times 10^7$	$0.89 \times 10^7$

columns (Case Bequ). Similar comparison was performed for Case C and equivalent piles located in between the position of columns (Case Cequ).

It was observed from Tables 10 and 11 that the maximum settlement and stress values reduced on the introduction of equivalent piles in the raft when compared to unpiled raft. Also, the settlement and stress values showed a very negligible variation in the cases between raft reinforced with regular piles and raft reinforced with equivalent pier for the two different pile layouts. The settlement and stress trend contours and magnitude also remained similar for the above two cases.

From Figs. 33 and 34, it was observed that the settlement and stress response pattern of the raft remained similar to other cases. It was observed that the variation in stresses and deformation between equivalent pier and piles was only about 2–5%. Thus, it can be concluded that equivalent piles can be used in the combined raft, pile and soil foundation system based on their availability.

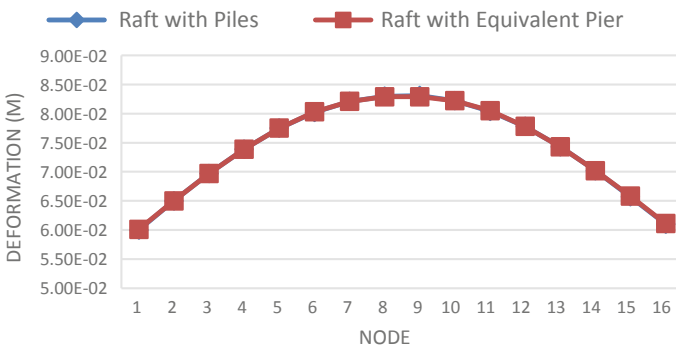


**Fig. 33** Comparison of raft deformation

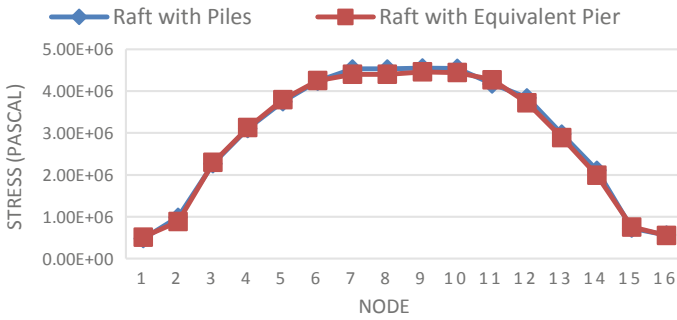


Fig. 34 Comparison of raft stresses

### 4 Conclusion

It was observed that the trend of settlement and stress variation in unpiled raft and piled raft for different layouts of piles was identical but with a variation in magnitude. The deformation reduced from 45–55% at the edges and 40–45% at the centre of the raft and the stress value reduced from 7–15% at the edges and 10–20% at the centre of the raft on an average due to the introduction of piles.

The load on the piles located at the centre of the raft was much higher than the piles positioned at other locations in the raft. The raft contact stresses obtained from the numerical analyses show uniform distribution except at the edges and pile locations. The stress distribution obtained from the numerical analysis indicated that the shaft stress is higher near the pile head and reduces towards the pile tip. The high stress at pile head was due to the transfer of raft stresses to the piles. It was also observed from the analyses that the tip stresses in piles were lesser than the head stresses indicating that the shaft friction was fully mobilized and the piles were dominantly friction piles. Also the mobilization of higher raft stress as the load increased and low pile tip stress at the final settlement confirms the behaviour of the pile group as settlement reducer (Cooke 1986, Fran 1991).

It was observed from the present study that the introduction of the piles not only reduced the raft settlement but also the stress level. Consequent to the reduction in stresses, the bending moment and the shear forces also get reduced. Thus, the study of raft stresses and bending moment along with the raft settlement leads to a better and effective design of the raft.

The variation in stresses and deformation between equivalent pier and general piles was only about 2–5%. Hence, equivalent pier system can also be used effectively based on requirement.

## References

- Balakumar V (2008) Experimental studies of model piled raft on sand and field study of proto type behaviour. Doctoral dissertation, PhD thesis, Anna University, Chennai
- Balakumar V, Huang M, Oh E, Balasubramaniam AS (2013a) Equivalent pier theory for piled raft design. In: Proceedings of the 18th international conference on soil mechanics and geotechnical engineering
- Balakumar V, Huang M, Oh E, Balasubramaniam AS (2013b) A design method for piled raft foundations. In: Proceedings of the 18th international conference on soil mechanics and geotechnical engineering, Paris, pp 2671–2674
- Cooke RW (1986) Piled raft foundation on stiff clays—a contribution to design philosophy. *Geotechnique* 36(2):169–203
- Fran E (1991) In: Measurements beneath piled rafts. Keynote lecture. ENPC conference Paris, pp 1–21
- Poulos HG (2001) Piled raft foundations: design and applications. *Geotechnique* 51(2):95–113
- Poulos HG (1994a) Alternative design strategies for piled raft foundations. In: Proceedings of the 3rd international conference deep foundations, Singapore, pp 239–244
- Poulos HG (1994b) An approximate numerical analysis of pile–raft interaction. *Int J Numer Anal Methods Geomech* 18(2):73–92
- Poulos HG (1998) The pile-enhanced raft—an economical foundation system. In: Proceedings, XI Brazilian conference on soil mechanics and geotechnical engineering, Brasília, vol 4, pp 27–43
- Zeevaert L (1957) Compensated friction pile foundation to reduce the settlement of buildings on highly compressible volcanic clay of Mexico city', In: Proceedings of the 14th international conference on soil mechanics and foundation engineerin, London (1957)